

## Analysis of the *VAV3* as Candidate Gene for Schizophrenia: Evidences From Voxel-Based Morphometry and Mutation Screening

Branko Aleksic<sup>1,2,†</sup>, Itaru Kushima<sup>1,2,†</sup>, Ryota Hashimoto<sup>2–4</sup>, Kazutaka Ohi<sup>2,4</sup>, Masashi Ikeda<sup>2,5</sup>, Akira Yoshimi<sup>1,2</sup>, Yukako Nakamura<sup>1,2</sup>, Yoshihito Ito<sup>1,2</sup>, Tomo Okochi<sup>2,5</sup>, Yasuhisa Fukuo<sup>2,5</sup>, Yuka Yasuda<sup>2,4</sup>, Motoyuki Fukumoto<sup>2,4</sup>, Hidenaga Yamamori<sup>2,4</sup>, Hiroshi Ujike<sup>6</sup>, Michio Suzuki<sup>2,7</sup>, Toshiya Inada<sup>2,8</sup>, Masatoshi Takeda<sup>2,4</sup>, Kozo Kaibuchi<sup>2,9</sup>, Nakao Iwata<sup>2,5,\*</sup>, and Norio Ozaki<sup>1,2</sup>

<sup>1</sup>Department of Psychiatry, Graduate School of Medicine, Nagoya University, Nagoya, Japan; <sup>2</sup>Core Research for Evolutional Science and Technology, Japan Science and Technology Corporation, Tokyo, Japan; <sup>3</sup>Molecular Research Center for Children's Mental Development, United Graduate School of Child Development, Osaka University, Kanazawa University and Hamamatsu University School of Medicine, Osaka, Japan; <sup>4</sup>Department of Psychiatry, Graduate School of Medicine, Osaka University, Osaka, Japan; <sup>5</sup>Department of Psychiatry, School of Medicine, Fujita Health University, 1-98 Dengakugakubo, Kutsukake-cho, Toyoake, Aichi 470-1192, Japan; <sup>6</sup>Department of Neuropsychiatry, Graduate School of Medicine, Dentistry and Pharmaceutical Sciences, Okayama University, Okayama, Japan; <sup>7</sup>Department of Neuropsychiatry, Graduate School of Medicine and Pharmaceutical Sciences, University of Toyama, Toyama, Japan; <sup>8</sup>Seiwa Hospital, Institute of Neuropsychiatry, Tokyo, Japan; <sup>9</sup>Department of Cell Pharmacology, Graduate School of Medicine, Nagoya University, Nagoya, Japan

†These authors contributed equally to this work.

\*To whom correspondence should be addressed; tel: 81-562-93-2000, fax: 81-562-93-1831, e-mail: nakao@fujita-hu.ac.jp

In recently completed Japanese genome-wide association studies (GWAS) of schizophrenia (JPN\_GWAS) one of the top association signals was detected in the region of *VAV3*, a gene that maps to the chromosome 1p13.3. In order to complement JPN\_GWAS findings, we tested the association of rs1410403 with brain structure in healthy individuals and schizophrenic patients and performed exon resequencing of *VAV3*. We performed voxel-based morphometry (VBM) and mutation screening of *VAV3*. Four independent samples were used in the present study: (1) for VBM analysis, we used case-control sample comprising 100 patients with schizophrenia and 264 healthy controls, (2) mutation analysis was performed on a total of 321 patients suffering from schizophrenia, and 2 case-control samples (3) 729 unrelated patients with schizophrenia and 564 healthy comparison subjects, and (4) sample comprising 1511 cases and 1517 healthy comparison subjects and were used for genetic association analysis of novel coding variants with schizophrenia. The VBM analysis suggests that rs1410403 might affect the volume of the left superior and middle temporal gyri ( $P = .011$  and  $P = .013$ , respectively), which were reduced in patients with schizophrenia compared with healthy subjects. Moreover, 4 rare novel missense variants were detected. The mutations were followed-up in large independent sample, and one of the novel variants (Glu741Gly) was associated with schizophrenia ( $P = .02$ ). These findings demonstrate that *VAV3* can be seen as novel candidate gene for schizophrenia in

which both rare and common variants may be related to increased genetic risk for schizophrenia in Japanese population.

*Key words:* resequencing/MRI/Japanese population/axon guidance/rare variant/GWAS

### Introduction

Schizophrenia is a severe mental disorder with a lifetime risk of about 1%, characterized by hallucinations, delusions, and cognitive deficits, with heritability estimated at up to 80%. Recently, there have been a few major advances in identifying common variants associated with schizophrenia by genome-wide association studies (GWAS). The GWAS approach has both highlighted genes previously identified by the candidate gene approach studies or by basic biological investigation and illuminated novel genomic loci clearly associated with schizophrenia that were previously unsuspected.<sup>1–3</sup>

In recently completed Japanese GWAS of schizophrenia (JPN\_GWAS),<sup>4</sup> one of the top association signals based on the meta-analysis for Japanese sample (rs1410403,  $P_{CMH} = 9.3 \times 10^{-4}$ , OR = 0.86) was detected in the region of *VAV3* (see online supplementary table 1). *VAV3* is closely related to the axon guidance pathways, which are implicated in etiology of schizophrenia.<sup>5</sup> During axon guidance, ephrin binding to Ephs triggers *VAV*-dependent endocytosis of the ligand-receptor

complex, converting an initially adhesive interaction into a repulsive event. In the absence of VAVs, ephrin-Eph endocytosis is blocked, leading to defects in growth cone collapse in vitro and significant defects in the ipsilateral retinogeniculate projections in vivo.<sup>6</sup> Therefore, VAV family guanine nucleotide exchange factors (GEFs) may play an important role as regulators of ligand-receptor endocytosis and determinants of repulsive signaling during axon guidance. The additional findings implicating the relevance of this locus for pathogenesis of schizophrenia came from genomewide linkage analysis of 236 Japanese families.<sup>7</sup> Specifically, they located the strongest evidence of linkage at rs2048839 (LOD [logarithm (base 10) of odds] = 3.39) and 95% CI comprises *VAV3* locus (Chr1: 102.0–111.9 Mbp, based on NCBI36 annotation).

Based on genetic evidence from the JPN\_GWAS, the meta-analysis for Japanese sample, biological studies, and linkage evidence *VAV3* can be seen as novel candidate gene for schizophrenia. Therefore, to follow-up JPN\_GWAS findings, we tested the association of rs1410403 with brain structure in healthy individuals and schizophrenic patients. Because biological phenotypes (eg, brain structure and function) are thought to more closely reflect the effects of genetic variation as compared with manifest psychiatric illness, endophenotype studies have proven to be more robust and require vastly smaller sample sizes than purely diagnosis-based studies.<sup>8</sup> Furthermore, statistical genetic association studies can provide a link between genes and complex polygenetic constructs like schizophrenia, but this approach does not illuminate the possible underlying pathophysiology impacted or the mechanisms of association. Here, we used imaging approach to examine the impact of variation in *VAV3* on risk for schizophrenia and function and structure in human brain of neural circuitries implicated in the pathophysiology of schizophrenia. Furthermore, in terms of genetic architecture, liability to schizophrenia is related to the number of loci involved and the effect size of each risk variant, and on the population level, these 2 factors combine to form an “allelic spectrum” which is bounded by “common disease/common variant” and “multiple rare variant” models.<sup>9</sup> Based on the results of recent schizophrenia GWAS, it was suggested that common variants can explain at least one-third of the total variation in liability, and genetic transmission patterns in schizophrenia may be a complex hybrid of common, low-penetrant alleles and rare, highly penetrant variants.<sup>1</sup> Therefore, in order to complement JPN\_GWAS findings and search for novel rare variants with larger effect, we performed exon resequencing of *VAV3*.

## Methods

### Sample

Four independent samples were used in the present study: (1) for the voxel-based morphometry (VBM) analysis, we

used case-control sample comprising 100 patients with schizophrenia ( $38.3 \pm 13.0$  y) and 264 healthy comparison subjects ( $36.7 \pm 11.9$  y), (2) mutation analysis was performed on a total of 321 patients suffering from schizophrenia ( $54.3 \pm 14.1$  y) (JMut sample) (3) JPN\_GWAS comprised of 729 unrelated patients with schizophrenia ( $45.4 \pm 15.1$  y) and 564 healthy comparison subjects ( $44.0 \pm 14.4$  y) and (4) Rep\_JPN comprising 1511 cases ( $45.9 \pm 14.0$  y) and 1517 healthy comparison subjects ( $46.0 \pm 14.6$  y). JPN\_GWAS and Rep\_JPN were used for genetic association analysis of novel coding variants with schizophrenia. The individuals with personal or family history of psychiatric disorders (first-degree relatives only based on the subject’s interview) were not included in the healthy comparison group. After complete description of the study to the subjects, written informed consent was obtained. A general characterization and psychiatric assessment of subjects are available elsewhere.<sup>10</sup>

### Voxel-Based Morphometry

All magnetic resonance (MR) studies were performed on a 1.5T GE Sigma EXCITE system. A 3-dimensional volumetric acquisition of a T1-weighted gradient echo sequence produced a gapless series of 124 sagittal sections using a spoiled gradient recalled acquisition in the steady state sequence (TE [Echo time]/TR [repetition time], 4.2/12.6 ms; flip angle, 15°; acquisition matrix, 256 × 256; 1NEX [number of excitations], FOV [Field of view], 24 × 24 cm; and slice thickness, 1.4 mm). Statistical analyses were performed with Statistical Parametric Mapping 5 (SPM5) software (<http://www.fil.ion.ucl.ac.uk/spm>) running on MATLAB R2007a (MathWorks, Natick, MA). MR images were processed using optimized VBM in SPM5 according to VBM5.1-Manual (<http://dbm.neuro.uni-jena.de/vbm/vbm5-for-spm5/manual/>) as described in detail previously.<sup>11,12</sup> Each image was confirmed to eliminate images with artifacts and then anterior commissure-posterior commissure line was adjusted. The normalized segmented images were modulated by multiplication with Jacobian determinants of the spatial normalization function to encode the deformation field for each subject as tissue density changes in the normal space. Finally, images were smoothed with a 12-mm full-width half-maximum of isotropic Gaussian kernel.

In first stage of the analysis, we performed whole brain search to explore the effects of diagnosis, genotype, and their interaction on gray matter (GM) volume in patients with schizophrenia and controls. These effects on GM volume were assessed statistically using the full factorial model for a 2 × 2 ANOVA in SPM5. We contrasted GM volumes between the genotype groups (individuals with A/A genotype and G-carriers), the diagnosis groups (smaller volume region in patients with schizophrenia relative to controls), and the diagnosis-genotype interaction. Age, sex, and education years were included to

control for confounding in all analyses. Because it is desirable to adjust for each subject's global GM volume,<sup>11</sup> adjustment was performed by entering the global GM values as a covariate. Nonsphericity estimation was used. These analyses yielded statistical parametric maps (SPM (*t*)) based on a voxel-level height threshold of  $P < .001$  (uncorrected for multiple comparisons). Only the clusters of more than 100 contiguous voxels were considered in the analyses. Additionally, small volume correction (SVC) was applied in order to protect against type I error using family wise error (FWE). The significance level was set  $P < 0.05$  (FWE corrected) after SVC, spheres with radius 10 mm around the peak.

In second stage of the analysis, we extracted a sphere of 10 mm volume of interest (VOI)-radius on left superior temporal gyrus and left middle temporal gyrus to compare regions of the genotype effects. Anatomic localization was according to both MNI coordinates and Talairach coordinates, obtained from M. Brett's transformations (<http://www.mrcbu.cam.ac.uk/Imaging/Common/mnispaces.html>) and presented as Talairach coordinates.

Statistical analyses were performed using PASW Statistics 18.0 software (SPSS Japan Inc., Tokyo, Japan). Differences in clinical characteristics between patients and controls or between genotypes were analyzed using  $\chi^2$  tests for categorical variables and the Mann-Whitney *U* test for continuous variables. We extracted the "y" values from the left superior temporal gyrus and left middle temporal gyrus maxima voxel and used these values in the VOI analysis using PASW. The effects of the variant in *VAV3* on extracted VOI were tested using the 2-way ANOVA without covariates because the extraction of VOI was performed after confounding factors, including age, sex, education years, and total GM volumes, were included in the whole-brain search analyses. Statistical significance was defined as  $P < .05$ .

### Mutation Screening

For the purpose of mutation screening, we have designed a custom resequencing microarray, based on NCBI36 build (Affymetrix, Santa Clara, CA), NAGOYA\_DESIGN, which primarily focuses on the genes selected, based on the JPN\_GWAS findings. The sequences tiled on the microarray included the sequences of all *VAV3* exons totaling 4933 bps (consensus CDS transcripts ENST00000370056 and ENST00000343258). Because the principle of the resequencing microarray is based on sequencing by hybridization, it was crucially important to avoid cross-hybridization to increase the accuracy of resequencing. For this purpose, we conducted an in-silico screening to compare the tiled sequences with a sliding 25-nucleotide window to detect the sequences with an

identity exceeding 22 bases in the tiled sequences and optimized the design of the microarrays and polymerase chain reaction (PCR) primers. Initially, the arrays were run according to the manufacturer's protocol. Briefly, long-range PCR conditions for the LA TaKaRa Polymerase (Takara, Japan) were: TaKaRa LA Taq 0.05 U/ $\mu$ l, 1X LA PCR Buffer II, 400  $\mu$ M (each) deoxynucleotide triphosphate, 0.3  $\mu$ M (each) primers, 4 ng/ $\mu$ l genomic DNA in a 25  $\mu$ l reaction volume. Modifications using standard approaches to PCR optimization were made for some difficult reactions. All PCR assays were quantified using PicoGreen (Molecular Probes, Eugene, OR) and then pooled in equimolar amounts. The PCR products were then purified, fragmented, labeled, and hybridized to the array. Finally, affymetrix GSEQ 4.0 Software (default settings) was used to process raw data and analyze the nucleotide sequences. SeqC Ver. 3.2.1.5 (JSI-medisys, [www.jsi-medisys.de](http://www.jsi-medisys.de)) was used to reanalyze the acquired datasets and assign annotation (based on NCBI 36 build). Novel variants with frequency of less than 5% were validated by cycle sequencing on ABI 3130xl DNA Analyzer (Applied Biosystems) according to standard manufacturer protocol. Allelic discrimination was performed using Taqman (Applied Biosystems) custom probes (details about DNA sequences, and PCR conditions are available upon request). Each 384 microtiter plate contained at least 3 nontemplate controls and the sample(s) in which novel variant was observed. Analysis was performed on HT7500 instrument (Applied Biosystems) according to the standard protocol. In-silico analysis of deleterious effect of amino acid substitution was done by algorithms implemented in LRT,<sup>13</sup> PMUT,<sup>14</sup> and PANTHER.<sup>15</sup> All these tools operate using approximately the same principles, that is, they are all supervised and employ features based on protein sequence, sequence conservation, and/or protein structure. The interpretation of the results was done based on score of the likelihood that missense variants, which cause a single amino acid substitution within a protein sequence, may or may not lead to altered protein function.

As basis for a more detailed functional interpretation of the novel rare variants, we performed ab-initio structure predictions based on I-TASSER algorithm.<sup>16</sup> This automated pipeline predicts secondary and tertiary protein structure based on sequence homology between protein/domain of interest and the proteins/domains with experimentally determined structures. The output of I-TASSER is analyzed and visualized using UCSF Chimera.<sup>17</sup>

All allele-wise association analyses were carried out by calculating the *P* values for each SNP using Fisher's exact test. In meta-analysis (JPN\_GWAS and Rep\_JPN sample), *P* values were generated by Cochran-Mantel-Haenszel stratified analysis. Two-tailed *P* values of less than 0.05 were considered significant. Calculations were done using Plink v1.07.<sup>18</sup>

**Table 1.** Demographic Information for Patients With Schizophrenia and Healthy Controls Included in the VBM Analysis

Variables <sup>a</sup>	Schizophrenia ( <i>N</i> = 100)					Control ( <i>N</i> = 264)					Group Difference <i>P</i> values ( <i>z</i> ) <sup>b</sup>		
	A/A		G-carrier			A/A		G-carrier					
	<i>(N</i> = 52)		<i>(N</i> = 48)			<i>(N</i> = 131)		<i>(N</i> = 133)					
	Mean	SD	Mean	SD	<i>P</i> values ( <i>z</i> ) <sup>b</sup>	Mean	SD	Mean	SD	<i>P</i> values ( <i>z</i> ) <sup>b</sup>			
Age (years)	37.7	12.5	39	13.5	0.91 (−0.12)	36.2	11.9	37.2	11.3	0.35 (−0.93)	0.37 (−0.89)		
Sex (male/female)	25/27		28/20			0.30 (1.05)	51/80		69/64			<b>0.035 (4.46)</b>	0.20 (1.66)
Education (years)	14.1	2.5	13.7	2.2	0.38 (−0.87)	14.9	2.1	15.3	2.4	0.21 (−1.26)	<b>&lt;0.001 (−4.13)</b>		
Estimated premorbid IQ	102.7	10.8	99.9	9.2	0.23 (−1.20)	107.4	8.6	106.9	7.6	0.58 (−0.55)	<b>&lt;0.001 (−5.07)</b>		
Gray matter volume (mm <sup>3</sup> )	666.2	73.1	688	82.6	0.23 (−1.20)	702.4	71.7	706.2	81.3	0.79 (−0.26)	<b>0.003 (−2.96)</b>		
CPZ-eq (mg/day) <sup>c</sup>	584.4	510.2	639.5	610.7	0.75 (−0.32)	—	—	—	—	—	—		
Age at onset (years)	25.5	10.6	25.1	10.9	0.91 (−0.11)	—	—	—	—	—	—		
Duration of illness (years)	12.2	10	13.9	10.7	0.37 (−0.90)	—	—	—	—	—	—		
PANSS positive symptoms	20.1	5.7	17.1	5.9	<b>0.009 (−2.61)</b>	—	—	—	—	—	—		
PANSS negative symptoms	19.8	6.4	18.3	6.2	0.13 (−1.50)	—	—	—	—	—	—		

Note: PANSS, Positive and Negative Syndrome Scale.

<sup>a</sup>Some demographic information was obtained in part of subjects (estimated premorbid IQ and PANSS in patients: A/A, *N* = 49; G-carriers, *N* = 46, Estimated premorbid IQ in controls: A/A, *N* = 130).

<sup>b</sup>Significant results are bolded and underlined.

<sup>c</sup>CPZ-eq: chlorpromazine equivalent of total antipsychotics.

## Results

### Voxel-Based Morphometry

We investigated effects of diagnosis, genotype, and their interaction on GM volumes in the whole brain analyses. There was no difference in demographic variables between *VAV3* genotype groups, except for scores of positive symptom between the genotype groups in patients with schizophrenia and sex between the genotype groups in healthy controls (table 1). Patients with schizophrenia showed reduced GM volumes compared with controls

mainly in the frontal lobe and temporal lobe (data not shown), consistent with previous studies.<sup>19,20</sup> Genotype effects on GM volume in several brain regions were found in all subjects (uncorrected *P* < .001, table 2). Individuals with A/A genotype had reduced GM volumes of left superior and middle temporal gyri than G-carriers, while individuals with A/A genotype had larger GM volumes of cerebellum anterior lobe (culmen) and right medial frontal gyrus than G-carriers (uncorrected *P* < .001, table 2). Additionally, we found significant diagnosis-genotype interaction of GM volume in the right medial frontal

**Table 2.** Effects of the *VAV3* Genotype on Brain Morphology in All Subjects

Brain regions	R/L	BA	Cluster Size	<i>T</i> <sub>356</sub>	<i>P</i> values <sup>a</sup>	Talairach Coordinates		
						<i>x</i>	<i>y</i>	<i>z</i>
A/A < G-carriers								
Superior temporal gyrus	L	13	194	3.8	<b>0.011</b>	−50	−48	18
Middle temporal gyrus	L	22	124	3.8	<b>0.013</b>	−53	−42	0
A/A > G-carriers								
Cerebellum anterior lobe (culmen)	R	NA	1533	4.1	<b>0.004</b>	7	−40	−12
Medial frontal gyrus	R	25	286	3.8	<b>0.012</b>	6	6	−17
<i>VAV3</i> genotype × diagnosis interaction								
Medial frontal gyrus	R	25	271	3.9	<b>0.009</b>	6	7	−18

Note: R, right; L, left; BA, brodmann area.

<sup>a</sup>Significant results (*P* < .05 [FWE corrected]) are indicated with bold and underline.

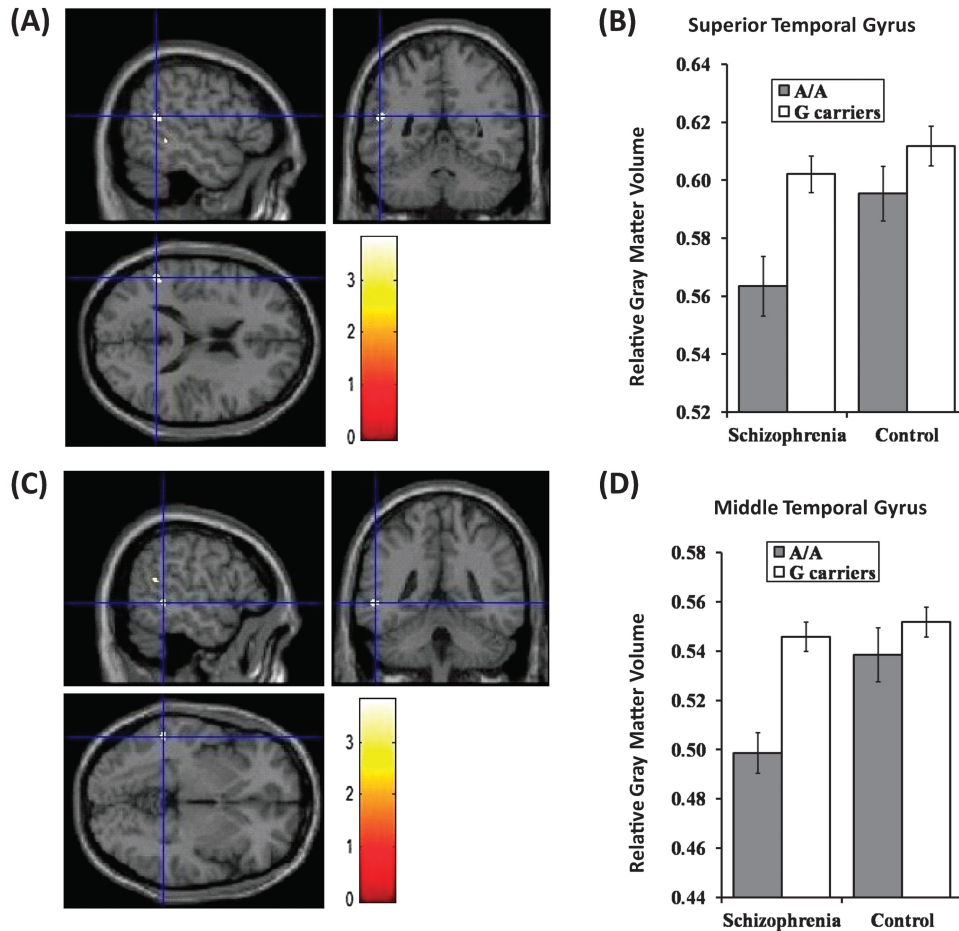


**Fig. 1.** Voxel-based morphometry. Impacts of VAV3 genotype on gray matter (GM) volumes of left superior temporal gyrus and left middle temporal gyrus. (A and C) Anatomical localizations were displayed on coronal, sagittal, and axial sections of a normal magnetic resonance imaging spatially normalized into the Montreal Neurological Institute template (uncorrected  $P < .001$ , cluster size  $> 100$ ). Significant clusters of genotype effect were in the left superior temporal gyrus (Talairach coordinate;  $-50, -48, 18$ ) (A) and in the left middle temporal gyrus ( $-53, -42, 0$ ) (C). These regions were showed as cross-hairline. The color bars showed  $t$  values corresponding to color in the figure. (B and D) Each column showed relative GM volumes extracted from left superior temporal gyrus ( $-50, -48, 18$ ) (B) and left middle temporal gyrus ( $-53, -42, 0$ ) (D). Data represent means  $\pm$  SEM.

gyrus (uncorrected  $P < .001$ , table 2). These results remained positive after SVC for multiple tests (FWE corrected  $P < .05$  after SVC).

Systematic searches for VBM studies have reported that smaller volumes of the left temporal gyrus were found in patients with schizophrenia than those in healthy subjects. Based on the JPN\_GWAS data, individuals with A/A genotype of the rs1410403 were enriched in patients with schizophrenia. Therefore, we focused on the individuals with A/A genotype of the rs1410403 in VAV3 as they may have a reduction of GM in the left superior temporal and left middle temporal gyri. Two-way ANOVA revealed significant effects of diagnosis ( $F_{1,360} = 5.77$ ,  $\eta^2 = 0.016$ ,  $P = .017$ ) and genotype ( $F_{1,360} = 10.04$ ,  $\eta^2 = 0.027$ ,  $P = .0017$ ) in the extracted region centering the left superior temporal gyrus ( $-50, -48, 18$ ) (figure 1A and B). No interaction was found in the left superior temporal gyrus ( $F_{1,360} = 1.65$ ,  $\eta^2 = 0.0046$ ,  $P = .20$ ). Individuals with homozygous A had smaller GM volumes of the left

superior temporal gyrus than G-carriers. We also found significant effects of diagnosis ( $F_{1,360} = 8.03$ ,  $\eta^2 = 0.022$ ,  $P = .0049$ ) and genotype ( $F_{1,360} = 14.04$ ,  $\eta^2 = 0.038$ ,  $P < .001$ ) and their interaction ( $F_{1,360} = 4.40$ ,  $\eta^2 = 0.012$ ,  $P = .037$ ) in the extracted region centering the left middle temporal gyrus ( $-53, -42, 0$ ) (figure 1C and D). As the genotype-diagnosis interaction was found in the left middle temporal gyrus, we analyzed the effects of genotype on the region in patients and controls separately. Patients with schizophrenia showed that patients with A/A genotype had smaller GM volumes of the region than G-carriers ( $F_{1,98} = 12.00$ ,  $\eta^2 = 0.11$ ,  $P < .001$ ). In contrast, controls showed no genotype effect on GM volumes of the region ( $F_{1,262} = 2.46$ ,  $\eta^2 = 0.0093$ ,  $P = .12$ ).

#### Mutation Screening

We detected 4 novel nonsynonymous heterozygous variants within the JMut sample (321 schizophrenic

patients). Protein homology analysis showed that VAV3 is highly conserved between species (~95% identical amino acids between human and mouse), accordingly the identified point mutations affected conserved residues (see online supplementary table 2). All the variants detected were located in the C-terminal region of VAV3 (see online supplementary figure 1).

The identified novel variants were reconfirmed by cycle sequencing and followed-up in 2 large independent schizophrenia case-control samples (Rep\_JPN and JPN\_GWAS sample). Only one rare variant (Glu741Gly) showed statistical evidence for association in meta-analysis ( $P_{CMH} = .020$ , OR = 0.58), while the others were observed at similar frequencies both in case and control samples (table 3). In-silico analysis of the missense variants applying 3 different algorithms predicted Glu741Gly as variant of functional relevance (table 4). Detailed 3-dimensional structural analysis of SH2 domain (wild type—figure 2a) indicated specific interaction (hydrogen bond) between Glu741 (side chain) and Lys735 (main chain). Point mutation at position 741 (Glu→Gly) would abolish hydrogen bonding because glycine does not contain a side chain (figure 2b). Moreover, beta strand extending into Lys735 is lost in the model of VAV3 mutant. The functional consequence of the associated point mutation is disappearance of casein kinase 2 phosphorylation site (SXXE)<sup>21</sup> as shown on figure 2c and d.

**Discussion**

Our study reports the systematic genetic evaluation of VAV3, as a candidate gene for schizophrenia based on our genome wide screening.<sup>4</sup> Specifically, meta-analysis of the JPN\_GWAS and follow-up sample provided genetic evidence for the involvement of VAV3 locus in schizophrenia in the Japanese population. Mutation screening of all VAV3 coding exons did not reveal evidence for the existence of a common (minor allele frequency >5%) nonsynonymous variant that explains the association signal in JPN\_GWAS.

The VBM analysis showed that the associated common SNP (rs1410403) might affect the volume of the left superior and middle temporal gyri, which were reduced in patients with schizophrenia compared with healthy subjects. VBM analysis suggests that VAV3's influence is focal to the aforementioned regions. Furthermore, the Allen Brain Atlas (<http://human.brain-map.org>) records relatively high levels of expression of the human VAV3 gene and lower expression levels of other VAV family GEFs (VAV1 or VAV2) in left superior and middle temporal gyri. Considering VAV3 biological function (developmental processes in particular), we speculate that our macroscopic observation using VBM approach is result of neuronal distribution and differential activity of VAV3 protein associated with rs1410403 genotypes.

**Table 3.** Resequencing Results

Chr	Variant	Physical Position <sup>a</sup>	Protein Domain	M	JMut (Minor Allele Count)	m	JPN_GWAS (MAF)			Rep_JPN (MAF)			Meta-Analysis			
							Cases	Control	$P_{allele}$	OR	Cases	Control	$P_{allele}$	OR	$P_{CMH}$	OR
1	p.Asp623Val	107,986,810	N-SH3	A	2	T	0.0006964	0.0008993	0.8561	0.7742	0.0003344	0	0.3171	NA	0.6649	1.662
1	p.Glu685Lys	107,947,271	SH2	G	1	A	0.0006974	0.001821	0.4151	0.3824	0.0003336	0	0.3168	NA	0.8415	0.8246
1	p.Glu705Lys	107,947,211	SH2	G	3	A	0.0007022	0.0009074	0.8557	0.7737	0.0006658	0.0003311	0.5605	2.011	0.7354	1.355
1	P.Glu741Gly	107,940,485	SH2	A	7	G	0.004972	0.01087	0.09038	0.4547	0.0074480	0.0117400	0.0897	0.6314	0.02065	0.5821

Note: M, major allele; m, minor allele; MAF, minor allele frequency; OR, odds ratio;  $P_{CMH}$ , Cochran-Mantel-Hentzel test.

<sup>a</sup>NCBI 36 build.

**Table 4.** In-Silico Analysis

Variant	Protein Domain	Genomic Data			Impact on Protein Structure/Function		
		Physical Position <sup>a</sup>	Strand	Alleles M/m	PMUT (Prediction Score) <sup>b</sup>	Panther (subPSEC Score) <sup>c</sup>	LRT ( <i>P</i> value) <sup>d</sup>
p.Asp623Val	N-SH3	Chr1: 107986810	-1	A/T	Yes (0.97)	Yes (-3.99)	Yes ( $4.29 \times 10^{-8}$ )
p.Glu685Lys	SH2	Chr1: 107947271	-1	G/A	Yes (0.93)	No (-2.04)	Yes ( $7.08 \times 10^{-10}$ )
p.Glu705Lys	SH2	Chr1: 107947211	-1	G/A	Yes (0.75)	No (-1.74)	Yes ( $1.83 \times 10^{-7}$ )
p.Glu741Gly	SH2	Chr1: 107940485	-1	A/G	Yes (0.89)	Yes (-3.24)	Yes ( $1.64 \times 10^{-6}$ )

Note: M/m, major/minor allele.

<sup>a</sup>NCBI36 build.

<sup>b</sup>>0.5 is interpreted as nonneutral substitution.

<sup>c</sup>Less than -3 is interpreted as nonneutral substitution.

<sup>d</sup><0.001 interpreted as nonneutral substitution.

Systematic searches for VBM studies have reported that reduced volumes of the left temporal gyrus were found in patients with schizophrenia.<sup>19</sup> Furthermore, the data from previous study of the superior temporal gyrus<sup>22</sup> and a study of the middle temporal gyrus in which patients with schizophrenia who were predisposed to auditory hallucinations showed reduced activation of the left middle temporal gyrus when imagining sentences in another person's voice.<sup>23</sup> Several other functional magnetic resonance imaging studies have reported decreased left and increased right middle temporal gyrus

activation in schizophrenia during auditory verbal hallucinations.<sup>24,25</sup> In our exploratory analysis (see online supplementary material), positive symptoms scores of Positive and Negative Syndrome Scale (PANSS) were not able to predict the VOIs in left superior and left middle temporal gyri ( $P > .05$ ). It is of note that VBM sample size in the current study might not be sufficient to detect the effect of positive symptoms score of PANSS on VOIs in left superior and left middle temporal gyri because positive symptoms score of PANSS is derived from symptomatology that is characterized by excess or distortion

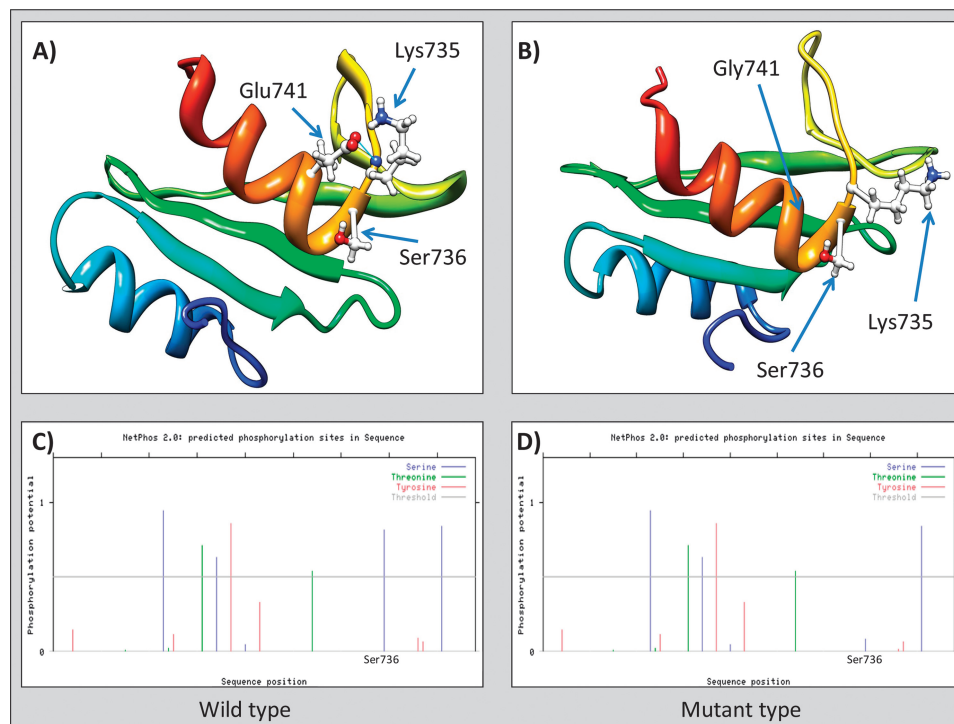


**Fig. 2.** Ab-initio 3D modeling of SH2 domain (VAV3). (a) Wild type, note hydrogen bond between Glu741 and Lys735 (blue line); (b) Mutant type, hydrogen bond between Gly741 and Lys735 cannot be formed; (c) and (d) phosphorylation potential of serine (blue), threonine (green), and tyrosine (red). Threshold is marked by horizontal gray line (phosphorylation analysis performed by NetPhos 2.0).

of the individual's normal functioning and therefore may not reflect only auditory hallucinations.

We detected several rare variants close to original association signal and in case of one rare variant (Glu741Gly), we observed nonsignificant association trend. When the evidence was combined across the 2 samples (JPN\_GWAS and Rep\_JPN sample), we found that the *P* values had strengthened. VAV3 is composed of 8 domains: calponin homology (CH), Acidic (Ac), Dbl homology (DH), pleckstrin homology (PH), zinc finger (ZF), Src homology 3 (SH3), Src homology 2 (SH2), and a second SH3 (see online supplementary figure 1).<sup>26</sup> Interestingly, the associated common variant (rs1410403) is located in LD block that encompass coding exons of SH2 domain of vav3 (see online supplementary figure 2), and the associated rare variant (Glu741Gly) is located within the exon that is translated into the SH2 domain of vav3 (see online supplementary figure 1).

VAV family GEFs have been implicated as regulators of Eph receptor endocytosis, the event which is required for efficient cell detachment.<sup>27</sup> This can provide a complex and dynamic set of cues that either repel or attract axons toward their synaptic targets, converting initially adhesive interaction into a repulsive force. Several studies had shown that SH2 domain of the VAV3 binds to phosphorylated tyrosine residue(s) on the EphA receptors,<sup>6,28</sup> which triggers endocytosis of EphA receptors and growth cone collapse.<sup>27</sup> Although the mechanisms by which Glu741Gly contributes to schizophrenia pathogenesis remain to be explored, we note that 3 different bioinformatics algorithms had predicted functional effect, and Glu741Gly have stronger protective effects on schizophrenia risk (OR = 0.58) than does the associated common SNP (OR = 0.81). Moreover, analysis of phosphorylation sites showed that point mutation at position 741 (Glu→Gly) would abolish phosphorylation of Ser736 by casein kinase II. The substitution of glutamic acid by Glycine at position 741 might have as a consequence alteration of the biological function of VAV3 because a substrate with *n* phosphorylation sites has an exponential number ( $2^n$ ) of phosphoforms and each phosphoform may have distinct properties.<sup>29</sup> Our genetic association results suggested that the rare variant, which is predicted to alter function of the VAV3, would decrease the risk of schizophrenia, whereas normal function is associated with schizophrenia. Same protective allelic effect was observed for common variant identified by JPN\_GWAS.

As the conclusion, our results showed that in case of schizophrenia, the “rare high-risk variant” vs the “common variant with low effect” hypotheses should not be viewed as 2 mutually exclusive hypotheses. Therefore, direct resequencing of candidate genes and copy number variants on the one side and GWAS analyses on the other side could be viewed as complementary approaches to analyze the genetic susceptibilities to schizophrenia.

## Funding

Funding for this study was provided by research grants from the Ministry of Education, Culture, Sports, Science and Technology of Japan; the Ministry of Health, Labor and Welfare of Japan; Grant-in-Aid for “Integrated research on neuropsychiatric disorders” carried out under the Strategic Research Program for Brain Sciences by the Ministry of Education, Culture, Sports, Science and Technology of Japan; Grant-in-Aid for Scientific Research on Innovative Areas (Comprehensive Brain Science Network) from the Ministry of Education, Science, Sports and Culture of Japan; The Academic Frontier Project for Private Universities, Comparative Cognitive Science Institutes, Meijo University; the Core Research for Evolutional Science and Technology and SENSHIN Medical Research.

## Supplementary Material

Supplementary material is available at <http://schizophreniabulletin.oxfordjournals.org>.

## Acknowledgments

The authors have no conflicts to declare.

## References

1. Purcell SM, Wray NR, Stone JL, et al. Common polygenic variation contributes to risk of schizophrenia and bipolar disorder. *Nature*. 2009;460:748–752.
2. Shi J, Levinson DF, Duan J, et al. Common variants on chromosome 6p22.1 are associated with schizophrenia. *Nature*. 2009;460:753–757.
3. Stefansson H, Ophoff RA, Steinberg S, et al. Common variants conferring risk of schizophrenia. *Nature*. 2009;460:744–747.
4. Ikeda M, Aleksic B, Kinoshita Y, et al. Genome-wide association study of schizophrenia in a Japanese population. *Biol Psychiatry*. 2011;69:472–478.
5. Yaron A, Zheng B. Navigating their way to the clinic: emerging roles for axon guidance molecules in neurological disorders and injury. *Dev Neurobiol*. 2007;67:1216–1231.
6. Cowan CW, Shao YR, Sahin M, et al. Vav family GEFs link activated Ephs to endocytosis and axon guidance. *Neuron*. 2005;46:205–217.
7. Arinami T, Ohtsuki T, Ishiguro H, et al. Genomewide high-density SNP linkage analysis of 236 Japanese families supports the existence of schizophrenia susceptibility loci on chromosomes 1p, 14q, and 20p. *Am J Hum Genet*. 2005;77:937–944.
8. Glahn DC, Thompson PM, Blangero J. Neuroimaging endophenotypes: strategies for finding genes influencing brain structure and function. *Hum Brain Mapp*. 2007;28:488–501.
9. Manolio TA, Collins FS, Cox NJ, et al. Finding the missing heritability of complex diseases. *Nature*. 2009;461:747–753.
10. Ikeda M, Aleksic B, Kirov G, et al. Copy number variation in schizophrenia in the Japanese population. *Biol Psychiatry*. 2010;67:283–286.



11. Good CD, Johnsrude IS, Ashburner J, et al. A voxel-based morphometric study of ageing in 465 normal adult human brains. *Neuroimage*. 2001;14:21–36.
12. Ashburner J, Friston KJ. Voxel-based morphometry—the methods. *Neuroimage*. 2000;11:805–821.
13. Chun S, Fay JC. Identification of deleterious mutations within three human genomes. *Genome Res*. 2009;19:1553–1561.
14. Ferrer-Costa C, Gelpi JL, Zamakola L, et al. PMUT: a web-based tool for the annotation of pathological mutations on proteins. *Bioinformatics*. 2005;21:3176–3178.
15. Thomas PD, Kejariwal A. Coding single-nucleotide polymorphisms associated with complex vs. Mendelian disease: evolutionary evidence for differences in molecular effects. *Proc Natl Acad Sci U S A*. 2004;101:15398–15403.
16. Roy A, Kucukural A, Zhang Y. I-TASSER: a unified platform for automated protein structure and function prediction. *Nat Protoc*. 2010;5:725–738.
17. Pettersen EF, Goddard TD, Huang CC, et al. UCSF Chimera—a visualization system for exploratory research and analysis. *J Comput Chem*. 2004;25:1605–1612.
18. Purcell S, Neale B, Todd-Brown K, et al. PLINK: a tool set for whole-genome association and population-based linkage analyses. *Am J Hum Genet*. 2007;81:559–575.
19. Chan RC, Di X, McAlonan GM, Gong QY. Brain anatomical abnormalities in high-risk individuals, first-episode, and chronic schizophrenia: an activation likelihood estimation meta-analysis of illness progression. *Schizophr Bull*. 2011;37:177–188.
20. Ellison-Wright I, Bullmore E. Anatomy of bipolar disorder and schizophrenia: a meta-analysis. *Schizophr Res*. 2010;117:1–12.
21. Aroor AR, Denslow ND, Singh LP, O'Brien TW, Wahba AJ. Phosphorylation of rabbit reticulocyte guanine nucleotide exchange factor in vivo. Identification of putative casein kinase II phosphorylation sites. *Biochemistry*. 1994;33:3350–3357.
22. Barta PE, Pearlson GD, Powers RE, Richards SS, Tune LE. Auditory hallucinations and smaller superior temporal gyral volume in schizophrenia. *Am J Psychiatry*. 1990;147:1457–1462.
23. McGuire PK, Silbersweig DA, Wright I, et al. Abnormal monitoring of inner speech: a physiological basis for auditory hallucinations. *Lancet*. 1995;346:596–600.
24. Woodruff P, Brammer M, Mellers J, et al. Auditory hallucinations and perception of external speech. *Lancet*. 1995;346:1035.
25. Lennox BR, Park SB, Medley I, Morris PG, Jones PB. The functional anatomy of auditory hallucinations in schizophrenia. *Psychiatry Res*. 2000;100:13–20.
26. Zugaza JL, Lopez-Lago MA, Caloca MJ, et al. Structural determinants for the biological activity of Vav proteins. *J Biol Chem*. 2002;277:45377–45392.
27. Bashaw GJ, Klein R. Signaling from axon guidance receptors. *Cold Spring Harb Perspect Biol*. 2010;2:a001941.
28. Hunter SG, Zhuang G, Brantley-Sieders D, et al. Essential role of Vav family guanine nucleotide exchange factors in EphA receptor-mediated angiogenesis. *Mol Cell Biol*. 2006;26:4830–4842.
29. Thomson M, Gunawardena J. Unlimited multistability in multisite phosphorylation systems. *Nature*. 2009;460:274–277.